ACS central science

Research Article

http://pubs.acs.org/journal/acscii

Quantitatively Resolving Ligand–Receptor Bonds on Cell Surfaces Using Force-Induced Remnant Magnetization Spectroscopy

Yi-Ting Chen, Andrew C. Jamison, T. Randall Lee,* and Shoujun Xu*

Department of Chemistry, University of Houston, Houston, Texas 77204, United States

Supporting Information

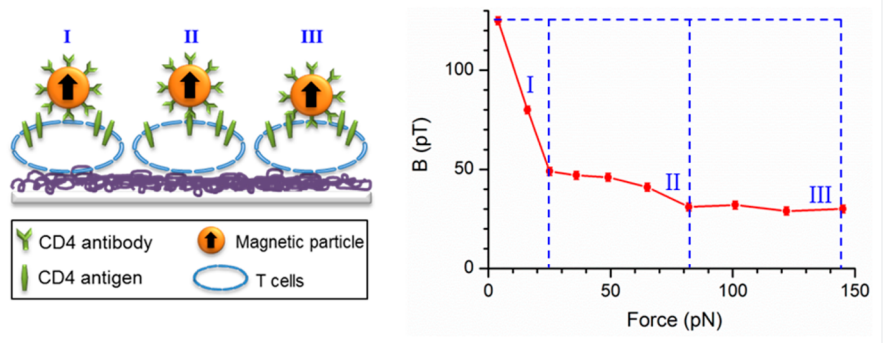

ABSTRACT: Molecule-specific noncovalent bonding on cell surfaces is the foundation for cellular recognition and functioning. A major challenge in probing these bonds is to resolve the specific bonds quantitatively and efficiently from the nonspecific interactions in a complex environment. Using force-induced remnant magnetization spectroscopy (FIRMS), we were able to resolve quantitatively three different interactions for magnetic beads bearing anti-CD4 antibodies with $CD4^+$ T cell surfaces based upon their binding forces. The binding force of the CD4 antibody–antigen bonds was determined to be 75 ± 3 pN. For comparison, the same bonds were also studied on a functionalized substrate surface, and the binding force was determined to be 90 ± 6 pN. The 15 pN difference revealed by high-resolution FIRMS illustrates the significant impact of the bonding environment. Because the force difference was unaffected by the cell number or the receptor density on the substrate, we attributed it to the possible conformational or local environmental differences of the CD4 antigens between the cell surface and substrate surface. Our results show that the high force resolution and detection efficiency afforded by FIRMS are valuable for studying protein–protein interactions on cell surfaces.

INTRODUCTION

The noncovalent bonds between ligand molecules and their corresponding receptors on a cell surface are important for cellular recognition and functioning.[1−3] Determining the various strengths of these noncovalent bonds is therefore critical for quantitatively evaluating the binding specificity and effect of drug molecules.[4] A challenging task is to identify and consequently eliminate interference from ubiquitous nonspecific absorption.[5,6] When single-molecule techniques are employed, a large number of measurements must be performed, and the measurements must be carefully filtered to obtain statistically significant results.[7,8] Therefore, these methods are limited by a low measuring efficiency. Nevertheless, atomic force microscopy (AFM) and optical tweezers have been extensively used to obtain force measurements of noncovalent bonds on substrate and cell surfaces, providing a wealth of information regarding the morphology of cell surfaces, configuration of molecules on surfaces, and cell surface receptor distribution.[9−12] Another challenge encountered with these studies is the accuracy of the force measurements, particularly when studying bonds under the equilibrium state. The current techniques usually produce a broad distribution range of binding forces, making it difficult to compare molecular bonds under different conditions.[13,14] In addition, most AFM studies concern the dynamic binding between the protein pair. It has been shown that the binding force varies with regard to the interaction time.[15] Therefore, to probe the equilibrium state of molecular bonds in an efficient manner, an alternative approach is needed.

Recently, we reported the development of force-induced remnant magnetization spectroscopy (FIRMS), which uses an external mechanical force to distinguish the specific molecular bonds from nonspecific physisorption.[16] The binding forces of noncovalent ligand–receptor bonds can be precisely determined by gradually increasing the mechanical force in the form of shaking,[16] centrifugal,[17] or acoustic input.[18] The general scheme is that the receptor molecules are immobilized on a surface, and the ligand molecules are labeled with magnetic beads. After applying the force at selected values, the overall magnetic signal of the beads is detected by a sensitive atomic magnetometer.[19−21] Bond dissociation is indicated by a

Received: September 30, 2015
Published: February 5, 2016

DOI: 10.1021/acscentsci.5b00325
ACS Cent. Sci. 2016, 2, 75−79

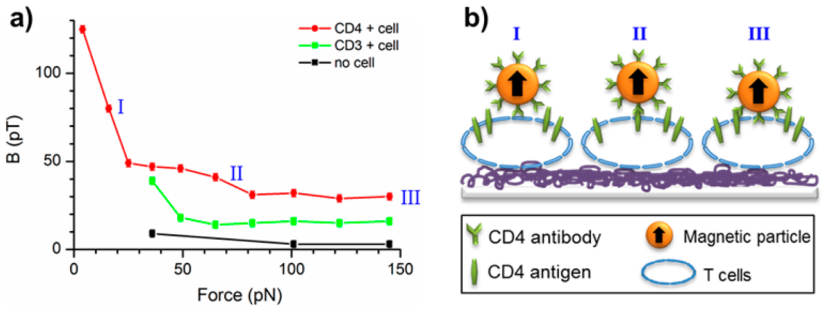

Figure 1. FIRMS results for the CD4 antibody–antigen interactions on cell surfaces. (a) Magnetic signal profile as a function of an external mechanical force revealing three different surface interactions (red trace). The green and black traces are control experiments as labeled. (b) Schematic illustration of the possible interactions between the anti-CD4 antibody-conjugated magnetic beads and $CD4^+$ T cells. The interaction types are I, weak nonspecific interactions; II, specific CD4 bonds; and III, stronger interactions.

decrease in the magnetic signal at a corresponding force value because the dissociated particles either will obtain random magnetic dipole orientations or will be removed from the sample system. The atomic magnetometer, located at several millimeters away from the sample, is mechanically separated from the magnetic beads. This detection method measures 10^4–10^5 bonds simultaneously. Its force resolution of ~2 pN allows for distinguishing different protein–protein bonds[18] and DNA duplexes having a single nucleotide difference.[17] However, prior to this work, the applications of FIRMS were limited to measuring molecular bonds on functionalized substrates. In this paper, we demonstrate quantitative measurements on cell surfaces for the first time.

Specifically, we show that the binding force of noncovalent ligand–receptor bonds on cell surfaces can be precisely determined by FIRMS and resolved from other interactions. We chose to study CD4 antibody–antigen bonds on the surface of $CD4^+$ T cells due to their significance in human immunodeficiency virus infection and cancers.[22,23] The expression of the CD4 antigen of this type of cell has been studied by flow cytometry[24] and mass spectrometry.[25] Additionally, AFM has been used to measure the binding force of the CD4 bonds on functionalized mica surfaces.[26] Our FIRMS results for measurements taken on cells and functionalized surfaces are compared under various conditions, with each other and with the existing results obtained using other techniques.

RESULTS AND DISCUSSION

Figure 1 shows a typical magnetic signal profile in a relatively wide force range of 0–144 pN for the anti-CD4 antibodies on the magnetic beads binding with the CD4 receptors on the cell surface. The two decreases in the profile, at approximately 25 and 82 pN, correspond to the dissociation of two different interactions. For this profile, the signal remains constant after 82 pN until the force limit, which indicates a strong interaction with a binding force exceeding 144 pN. These observations allow us to divide the profile into three regions as indicated in Figure 1a. The first, region I (between 0 and 25 pN), represents the nonspecific binding between the antibody-conjugated magnetic beads and the cell surface, which has been well documented in both of our previous works[16,17] and single-molecule studies.[5,15] The second region of decreased signal, region II between 50 and 82 pN, is assigned to the dissociation of the specific bonds between anti-CD4 antibody and CD4 antigen (referred to as CD4 bonds hereafter). To confirm this assignment, we performed two control experiments in which there were either no cells or no matching antibodies on the magnetic beads. In the latter case, the beads were conjugated with a CD3 antibody. No signal decrease was observed at 50–82 pN for either case (Figure 1, green and black traces). Therefore, we concluded that CD4 bonds have a binding force in region II. The third region, region III (above 82 pN), is associated with stronger bonding than the CD4 bonds, which also existed between CD3 antibody-conjugated beads and the cell surface. We attribute the continued presence of bound magnetic beads to possible multiple bonds or strong nonspecific interactions similar to studies using AFM or magnetic tweezers.[3,27–29] The three different interactions are schematically illustrated in Figure 1b. We note that the binding force for the biotin–streptavidin bonds is approximately 250 pN,[27] which then should not interfere with the assignment of the three regions for the CD4 bonds.

The signal amplitude of each region provides the quantity of the magnetic beads bound through the corresponding interaction. Our primary interest in this work centers on the 18 pT decrease in region II that belongs to the CD4 bonds. Based on the calibration of the magnetic signal vs the number of beads,[17] the 18 pT signal corresponds to 5.4×10^4 magnetically labeled CD4 bonds. The majority of the initial magnetic signal correlates to the weak nonspecific binding, which was 77 pT of the initial 126 pT; leaving 31 pT for the remaining stronger interaction. Therefore, the specific CD4 bonds only comprised ~14% of the total possible surface interactions. This percentage is consistent with the binding probabilities obtained by AFM and other force techniques.[5,6,15] The difference, however, is that FIRMS captures all of the interactions in a single measurement, whereas AFM requires hundreds of repeated measurements or more.

Optical imaging by a microscope was used to verify the immobilization of the cells and to determine the cell density. The images of the sample were taken before and after the forces were applied. Cell counting for the same sizes of field of view of 0.04 mm^2 yielded 242 ± 16 and 250 ± 8, respectively. The similar numbers confirm the successful immobilization of the cells. The residual magnetic beads (black dots) in Figure 2b correspond to the strongly bound magnetic particles after application of the 144 pN force (conclusion of region III in Figure 1). Because the overall surface area of the sample well is 7 mm^2, we calculate the total number of cells to be 4.3×10^4. The average size of the cells is estimated to be 5.3 μm in diameter from the SEM images. Therefore, the surface coverage of the cells is approximately 15%.

DOI: 10.1021/acscentsci.5b00325
ACS Cent. Sci. 2016, 2, 75–79

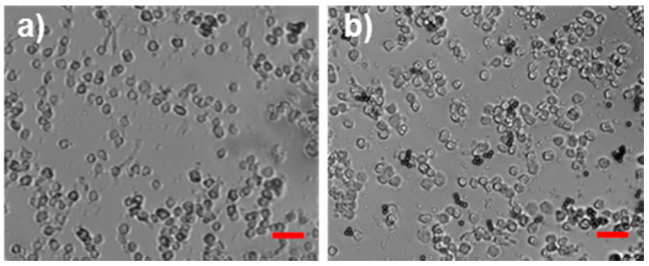

Figure 2. Optical images of the $CD4^+$ T cell decorated surfaces. (a) Before incubating with magnetic beads and applying mechanical force and (b) after FIRMS measurements. Scale bars: 20 μm.

To determine the binding force of the specific CD4 bonds, we performed measurements in a narrower force range of 50−120 pN at smaller force increments. For comparison, the same bonds were also studied on a CD4 antigen-functionalized gold substrate. The resulting magnetic signal profiles are presented in Figure 3, with their corresponding force spectra shown in the

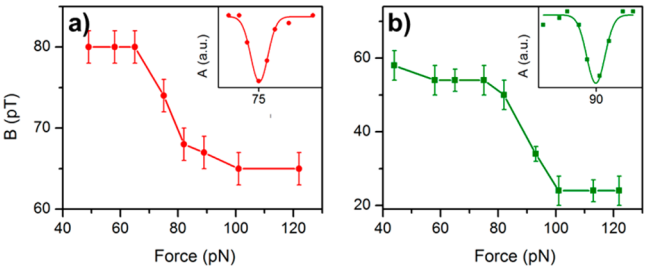

Figure 3. High-resolution analysis of the binding forces of the CD4 bonds. (a) Results for the $CD4^+$ T cell surface. (b) Results for the CD4 antigen-functionalized substrate. Insets are the Gaussian fittings of the corresponding force spectra.

insets. The force spectra were obtained by taking the derivative of the corresponding magnetic signal profiles. The precise binding forces were extracted from the Gaussian fittings of the force spectra, which were 75 ± 3 pN for the cell surface and 90 ± 6 pN for the CD4 antigen-functionalized gold substrate. Control experiments were performed to confirm the specific bonds on the gold surface (Figure S1). Measurements for each case were repeated four times, and similar binding forces were obtained for each surface type (Figure S2). The error bars of the force values are the respective standard deviations of the measurements. The value we obtained on the functionalized substrate is consistent with the mean value of 79 ± 59 pN obtained by AFM,[26] but with much improved force certainty.

The high force resolution of FIRMS reveals a new observation that the CD4 bonds are substantially weaker on the cell surface than they are on the functionalized substrate surface. There are several possible reasons that might explain the reduced binding force, such as differences in antigen conformation or local environment, cell counts on the surface, and antigen densities on the substrate. To examine possible reasons for the force difference, we attempted to reduce the cell number and to reduce the antigen density on the substrate. The resulting force measurements are shown in Figure 4. For the reduced cell number, the binding force was determined to be 70 ± 5 pN, which showed no difference from the result for the higher cell number. The associated SEM image shows that, under this condition, the cells were well separated on the surface, eliminating most of the cell−cell interactions and the

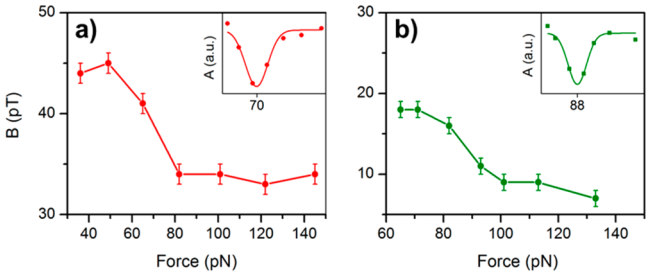

Figure 4. Plots of the remnant magnetization as a function of the binding force under different conditions. (a) Results on the $CD4^+$ T cell decorated surface with fewer cells. (b) Results on the CD4 antigen-functionalized substrate with reduced antigen density. Insets are the Gaussian fittings of the corresponding force spectra.

potential effect on the CD4 bonds (Figure S3). Cell counting for the image yielded an estimated total of 2.4×10^4 cells in the sample, or ∼56% of the initial cell density. Separately, we achieved a reduced antigen density on the functionalized substrate by using a mixture of tetradecanethiol and mercaptohexadecanoic acid (4:1 ratio) to dilute the carboxylic acid groups on the surface. The result in Figure 4b shows the same binding force of 88 ± 7 pN as the 90 ± 6 pN obtained for the higher antigen density in Figure 3b. Note that the overall signal was much lower because of the reduced amount of antigen molecules on the surface. Further dilution until there was barely any magnetic signal, in which the tetradecanethiol to mercaptohexadecanoic acid ratio is 10:1, showed that the binding force remained the same (Figure S4). To quantify the low densities of the surface antigen, we carried out an X-ray photoelectron spectroscopy study that produced results consistent with the magnetic measurements (Supporting Information and Figure S5). These experiments confirmed that the differences in the binding force between the cell surface and the functionalized substrate are due neither to cell−cell interactions nor to the neighboring bonds on the substrate. In contrast, the most plausible rationalization for the observed different binding strengths is that the CD4 antigens adopt different conformations or experience different environments on the surface of the cells as compared to the functionalized substrate.

In addition to the high force resolution, the capability of FIRMS to reveal the total number of molecular bonds enables us to determine the maximum number of CD4 bonds under our experimental conditions. In Figure 5, we varied the amount of magnetic beads, but maintained a constant number of cells on each sample. The magnetic signal of the CD4 bonds reached

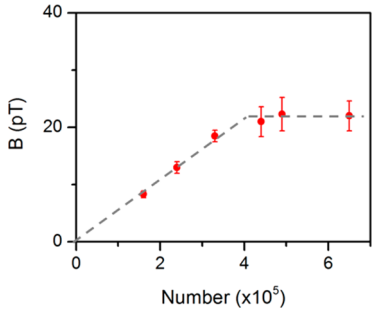

Figure 5. Plot of the magnetic signal corresponding to the CD4 bonds at various numbers of magnetic beads. Saturation was observed at 4.1 × 10^5 particles.

DOI: 10.1021/acscentsci.5b00325
ACS Cent. Sci. 2016, 2, 75−79

a plateau at 4.1 × 10^5 beads; further increasing the bead number had no effect on the signal. The maximum signal was 22 pT, corresponding to 6.7 × 10^4 CD4 bonds. This result indicates that, on average, each cell formed more than one but less than two single CD4 bonds for the given sizes of the beads and cells. This observation is consistent with the results in Figure 1 in which the specific antibody−antigen bonds represented only a small portion of all three types of interactions between the magnetically labeled antibody molecules and antigens on the cells. However, we could not provide information regarding the actual distribution of the number of particles on individual cells. The quantification and resolution of molecular bonds in our system are important for many applications, such as using nano- and microparticles as drug carriers to target specific types of cells.[30,31] Furthermore, the capability of FIRMS to measure a large surface area to determine the total number of molecular bonds complements the limited field of view of single molecule-based force techniques such as AFM and optical tweezers.

CONCLUSIONS

We have shown that FIRMS is capable of resolving the noncovalent molecular bonds on cell surface with precise force resolution and high detection efficiency. The binding force of the CD4 bonds on $CD4^+$ T cells was revealed to be 75 ± 3 pN, which is 15 pN lower than the same type of bond on a CD4 antigen-functionalized gold substrate. We verified that this difference depends neither on the cell number nor the coating density on the substrate surface. Because of this substantial difference, our results suggest that it is necessary to study protein−protein bonds directly on cell surfaces when possible. This research has further demonstrated that the FIRMS technique has the potential to reveal the behavior of protein−protein bonds during various biological processes such as cell functioning and drug targeting. Our research is currently exploring related phenomena in living cells.

EXPERIMENTAL METHODS

Materials. $CD4^+$ T cells were purchased from Innovative Research and preserved according to the manufacturer's instructions (details provided in the Supporting Information). CD4 recombinant human protein (PHS0044), CD3D and CD3E recombinant human protein (10981-H08H), magnetic beads functionalized with streptavidin (Dynabeads M280), and phosphate-buffered saline (PBS, pH = 7.4) were purchased from Invitrogen. Bovine serum albumin (BSA), monoclonal biotinylated human CD3 antibody produced in mouse (SHAB4700047), poly(L-lysine) (PLL) (0.1%, w/v, molecular weight 150,000−300,000), glutaraldehyde (25 wt % in H_2O), tetradecanethiol, 16-mercaptohexadecanoic acid (98%), *N*-hydroxysuccinimide (NHS), and *N*-(3-(dimethylamino)-propyl)-*N*′-ethylcarbodiimide hydrochloride (EDC) were purchased from Sigma-Aldrich. The 0.5 M EDTA solution obtained from Ambion was used as received. Biotinylated anti-CD4 antibody (MEM-241) was obtained from Abcam. Isolation buffer was prepared from PBS with 0.1% BSA and 2 mM EDTA.

Sample Preparation for CD4 Binding on Cell Surfaces. Glass slides were cleaned and incubated with 0.01% (w/v) PLL solution for 30 min. The PLL-coated glass slides were then rinsed with Milli-Q water and dried under nitrogen. The sample well was assembled by gluing the glass to a 20 × 3 × 1 mm^3 ($L \times W \times H$) polystyrene piece with a 4 mm × 2 mm oval opening at the center (area 7 mm^2). The $CD4^+$ T cells were washed twice with PBS buffer and diluted to the desired concentrations. The cell concentration was determined by a hemocytometer. To immobilize the cells on the PLL coating,[32] 7 μL of cell suspension in PBS buffer was placed in contact with the surface for 15 min, followed by adding 3 μL of a mixture of 3.5% (w/v) paraformaldehyde and 1% (w/v) glutaraldehyde in water overnight. The cells were presumably dead after fixation. After rinsing with PBS buffer three times, the sample well was immersed in 3% (w/w) BSA solution to reduce nonspecific interactions. Conjugation of the streptavidin-functionalized magnetic beads with the biotinylated anti-CD4 antibody was carried out at room temperature for 1 h. Finally, 7 μL of the magnetic beads (diluted by 20 times) conjugated with the anti-CD4 antibody was introduced to the sample well, incubated for 3 h, and magnetized by a permanent magnet (0.5 T).

Sample Preparation for CD4 Binding on a Functionalized Surface. The sample well was assembled by attaching a gold-coated glass slide (Evaporated Coatings, Inc.) to the same polystyrene piece used in the previous section. The gold surface was initially functionalized with carboxylic acid groups by incubating the surface in a 3 mM ethanolic solution of 16-mercaptohexadecanoic acid for 24 h. For reduced functionalization densities, tetradecanethiol was mixed with mercaptohexadecanoic acid at 4:1 and 10:1 ratios, respectively. The functionalized surface then reacted with 7 μL of aqueous mixture containing 0.05 M NHS and 0.2 M EDC. Then the sample well was incubated with the CD4 antigen in PBS for 4 h, followed by exchanging the protein solution with PBS buffer several times before incubation of 3% (w/w) BSA for 1 h to minimize nonspecific interactions.[33] After that, 7 μL of the magnetic beads conjugated with anti-CD4 antibody was introduced to the sample well and then magnetized.

FIRMS Measurements. Measurements of the magnetic signals of the sample were obtained using an atomic magnetometer,[21] which has a noise level of ∼1−2 pT in this work. Mechanical forces of varying amplitudes were produced by a centrifuge (Eppendorf 5417R) at various speeds. The force amplitude was calculated based on the equation $F = m\omega^2 r$, where m is the buoyant mass of the beads (4.6 × 10^{-15} kg, determined in previous work), ω is the centrifuge angular velocity, and r is the distance of the sample from the rotation center (8 cm in this work).[17,34] The remnant magnetization of the magnetic beads was subsequently measured after each application of centrifugal force using a scanning method that we previously reported.[35] More details are provided in the Supporting Information, with Figure S6.

ASSOCIATED CONTENT

Supporting Information

The Supporting Information is available free of charge on the ACS Publications website at DOI: 10.1021/acscentsci.5b00325.

Experimental method, control experiments, force measurement statistics, image of the cells at reduced density, XPS analysis, and Figures S1−S6 (PDF)

AUTHOR INFORMATION

Corresponding Authors

*E-mail: trlee@uh.edu (T.R.L.).
*E-mail: sxu7@uh.edu (S.X.).

DOI: 10.1021/acscentsci.5b00325
ACS Cent. Sci. 2016, 2, 75−79

Notes

The authors declare no competing financial interest.

■ ACKNOWLEDGMENTS

This work was supported by the National Science Foundation under Grant No. ECCS-1508845 (S.X.). Additional support was provided to T.R.L. and S.X. by the Texas Center of Superconductivity at the University of Houston (TcSUH) and to T.R.L. by the Robert A. Welch Foundation (Grant No. E-1320).

■ REFERENCES

(1) Bai, R.; Yi, S.; Zhang, X.; Liu, H.; Fang, X. Role of ICAM-1 polymorphisms (G241R, K469E) in mediating its single-molecule binding ability: Atomic force microscopy measurements on living cells. *Biochem. Biophys. Res. Commun.* **2014**, *448*, 372−378.

(2) Pillet, F.; Chopinet, L.; Formosa, C.; Dague, É. Atomic force microscopy and pharmacology: From microbiology to cancerology. *Biochim. Biophys. Acta, Gen. Subj.* **2014**, *1840*, 1028−1050.

(3) Lekka, M.; Laidler, P.; Łabędź, M.; Kulik, A. J.; Lekki, J.; Zając, W.; Stachura, Z. Specific detection of glycans on a plasma membrane of living cells with atomic force microscopy. *Chem. Biol.* **2006**, *13*, 505−512.

(4) Yu, J.; Wang, Q.; Shi, X.; Ma, X.; Yang, H.; Chen, Y.-G.; Fang, X. Single-molecule force spectroscopy study of interaction between transforming growth factor b_1 and its receptor in living cells. *J. Phys. Chem. B* **2007**, *111*, 13619−13625.

(5) Gilbert, Y.; Deghorain, M.; Wang, L.; Xu, B.; Pollheimer, P. D.; Gruber, H. J.; Errington, J.; Hallet, B.; Haulot, X.; Verbelen, C.; Hols, P.; Dufrêne, Y. F. Single-molecule force spectroscopy and imaging of the vancomycin/D-ala/D-ala interaction. *Nano Lett.* **2007**, 7 (3), 796−801.

(6) Sitters, G.; Kamsma, K.; Thalhammer, G.; Ritsch-Marte, M.; Peterman, E. J. G.; Wuite, G. J. L. Acoustic force spectroscopy. *Nat. Methods* **2015**, *12*, 47−50.

(7) Dufrêne, Y. F.; Evans, E.; Engel, A.; Helenius, J.; Gaub, H. E.; Müller, D. J. Five challenges to bringing single-molecule force spectroscopy into living cells. *Nat. Methods* **2011**, *8*, 123−127.

(8) Friedrichs, J.; Legate, K. R.; Schubert, R.; Bharadwaj, M.; Werner, C.; Müller, D. J.; Benoit, M. A practical guide to quantify cell adhesion using single-cell force spectroscopy. *Methods* **2013**, *60*, 169−178.

(9) McEwen, G. D.; Wu, Y.; Tang, M.; Qi, X.; Xiao, Z.; Baker, S. M.; Yu, T.; Gilbertson, T. A.; DeWald, D. B.; Zhou, A. Subcellular spectroscopic markers, topography and nanomechanics of human lung cancer and breast cancer cells examined by combined Raman microspectroscopy and atomic force microscopy. *Analyst* **2013**, *138*, 787−797.

(10) Alsteens, D.; Dupres, V.; Yunus, S.; Latgé, J.-P.; Heinisch, J. J.; Dufrêne, Y. F. High-resolution imaging of chemical and biological sites on living cells using peak force tapping atomic force microscopy. *Langmuir* **2012**, *28*, 16738−16744.

(11) Almqvist, N.; Bhatia, R.; Primbs, G.; Desai, N.; Banerjee, S.; Lal, R. Elasticity and adhesion force mapping reveals real-time clustering of growth factor receptors and associated changes in local cellular rheological properties. *Biophys. J.* **2004**, *86*, 1753−1762.

(12) Zhang, J.; Wu, G.; Song, C.; Li, Y.; Qiao, H.; Zhu, P.; Hinterdorfer, P.; Zhang, B.; Tang, J. Single molecular recognition force spectroscopy study of a luteinizing hormone-releasing hormone analogue as a carcinoma target drug. *J. Phys. Chem. B* **2012**, *116*, 13331−13337.

(13) O'Donoghue, M. B.; Shi, X.; Fang, X.; Tan, W. Single-molecule atomic force microscopy on live cells compares aptamer and antibody rupture forces. *Anal. Bioanal. Chem.* **2012**, *402*, 3205−3209.

(14) Lee, C.-K.; Wang, Y.-M.; Huang, L.-S.; Lin, S. Atomic force microscopy: Determination of unbinding force, off rate and energy barrier for protein-ligand interaction. *Micron* **2007**, *38*, 446−461.

(15) Dupres, V.; Menozzi, F. D.; Locht, C.; Clare, B. H.; Abbott, N. L.; Cuenot, S.; Bompard, C.; Raze, D.; Dufrêne, Y. F. Nanoscale mapping and functional analysis of individual adhesins on living bacteria. *Nat. Methods* **2005**, *2*, 515−520.

(16) Yao, L.; Xu, S.-J. Force-induced remnant magnetization spectroscopy for specific magnetic imaging of molecules. *Angew. Chem., Int. Ed.* **2011**, *50*, 4407−4409.

(17) De Silva, L.; Yao, L.; Wang, Y.; Xu, S.-J. Well-defined and sequence-specific noncovalent binding forces of DNA. *J. Phys. Chem. B* **2013**, *117*, 7554−7558.

(18) De Silva, L.; Yao, L.; Xu, S.-J. Mechanically resolving noncovalent bonds using acoustic radiation force. *Chem. Commun.* **2014**, *50*, 10786−10789.

(19) Budker, D.; Romalis, M. V. Optical magnetometry. *Nat. Phys.* **2007**, *3*, 227−234.

(20) Kominis, I. K.; Kornack, T. W.; Allred, J. C.; Romalis, M. V. A subfemtotesla multichannel atomic magnetometer. *Nature* **2003**, *422*, 596−599.

(21) Garcia, N. C.; Yu, D.; Yao, L.; Xu, S.-J. Optical atomic magnetometer at body temperature for magnetic particle imaging and nuclear magnetic resonance. *Opt. Lett.* **2010**, *35*, 661−663.

(22) Harrison, S. C. CD4: Structure and interactions of an immunoglobulin superfamily adhesion molecule. *Acc. Chem. Res.* **1993**, *26*, 449−453.

(23) Hu, M.; Wang, J.; Cai, J.; Wu, Y.; Wang, X. Nanostructure and force spectroscopy analysis of human peripheral blood $CD4^+$ T cells using atomic force microscopy. *Biochem. Biophys. Res. Commun.* **2008**, *374*, 90−94.

(24) Davis, K. A.; Abrams, B.; Iyer, S. B.; Hoffman, R. A.; Bishop, J. E. Determination of CD4 antigen density on cells: Role of antibody valency, avidity, clones, and conjugation. *Cytometry* **1998**, *33*, 197−205.

(25) Wang, M.; He, H.-J.; Turko, I. V.; Phinney, K. W.; Wang, L. Quantifying the cluster of differentiation 4 receptor density on human T lymphocytes using multiple reaction monitoring masss spectrometry. *Anal. Chem.* **2013**, *85*, 1773−1777.

(26) Chen, Y.; Zeng, G.; Chen, S. S.; Feng, Q.; Chen, Z. W. AFM force measurements of the gp120-sCD4 and gp120 or CD4 antigen-antibody interactions. *Biochem. Biophys. Res. Commun.* **2011**, *407*, 301−306.

(27) Wong, S. S.; Joselevich, E.; Woolley, A. T.; Cheung, C. L.; Lieber, C. M. Covalently functionalized nanotubes as nanometre-sized probes in chemistry and biology. *Nature* **1998**, *394*, 52−55.

(28) Mammen, M.; Choi, S.-K.; Whitesides, G. M. Polyvalent interactions in biological systems: Implications for design and use of multivalent ligands and inhibitors. *Angew. Chem., Int. Ed.* **1998**, *37*, 2754−2794.

(29) Jacob, A.; van IJzendoorn, L. J.; de Jong, A. M.; Prins, M. W. J. Quantification of protein-ligand dissociation kinetics in heterogeneous affinity assays. *Anal. Chem.* **2012**, *84*, 9287−9294.

(30) Martinez-Veracoechea, F. J.; Frenkel, D. Designing super selectivity in multivalent nano-particle binding. *Proc. Natl. Acad. Sci. U. S. A.* **2011**, *108*, 10963−10968.

(31) Li, M.-H.; Choi, S. K.; Leroueil, P. R.; Baker, J. R., Jr. Evaluating binding avidities of populations of heterogeneous multivalent ligand-functionalized nanoparticles. *ACS Nano* **2014**, *8*, 5600−5609.

(32) Sen, S.; Subramanian, S.; Discher, D. E. Indentation and adhesive probing of a cell membrane with AFM: Theoretical model and experiments. *Biophys. J.* **2005**, *89*, 3203−3213.

(33) Lahiri, J.; Isaacs, L.; Tien, J.; Whitesides, G. M. A strategy for the generation of surfaces presenting ligands for studies of binding based on an active ester as a common reactive intermediate: a surface plamon resonance study. *Anal. Chem.* **1999**, *71*, 777−790.

(34) Halvorsen, K.; Wong, W. P. Massively parallel single-molecule manipulation using centrifugal force. *Biophys. J.* **2010**, *98*, L53−L55.

(35) Yao, L.; Xu, S.-J. Long-range, high-resolution magnetic imaging of nanoparticles. *Angew. Chem., Int. Ed.* **2009**, *48*, 5679−5682.

DOI: 10.1021/acscentsci.5b00325
ACS Cent. Sci. 2016, 2, 75−79